



Cold-Formed Steel – Research to Practice

Roger A. LaBoube¹

Abstract

Research studies at the University of Missouri-Rolla have focused on developing a better understanding of the behavior of cold-formed steel members and assemblies. This research was initiated by the more widespread use of cold-formed steel in the construction market, and the need to provide structurally reliable, as well as highly economical design solutions. This paper summarizes several of my student's studies, and the suggested design recommendations.

1. Introduction

In the United States, the use of cold-formed steel sections as framing members has gained an increased acceptance in the construction market. Cold-formed steel members and assemblies have been widely used in commercial and industrial construction applications.

At the University of Missouri-Rolla (UMR), research studies to better define the behavior and design of cold-formed steel members and assemblies as well as connections using bolts, screws and welds have been completed. Much research at UMR and other universities has focused on member behavior but to obtain more economical cold-formed steel design solutions for the construction industry the future research efforts should focus on the behavior of assemblies.

This paper provides a summary of research studies that focused on cold-formed steel assemblies to include built-up I-sections, trusses and header beams. The design guidelines developed from the research were implemented by incorporation into the *North American Standard for Cold-Formed Steel Framing* (American, 2015).

2. Built-up I Sections

An experimental investigation was conducted to study the behavior of built-up cold-formed steel I-sections and to determine if the modified slenderness ratio in the AISI specification (American, 2012) is valid for cold-formed steel members. Typical I-section applications include framing for windows, doorways, shear walls and multi-story cold-formed steel framed buildings in which the lower floor framing utilizes built-up studs to carry the load. The built-up studs that were studied

¹ Curators' Teaching Professor Emeritus and Director of the Wei-Wen Yu Center for Cold-Formed Steel Structures, Missouri University of Science and Technology, <laboube@mst.edu>

consisted of two C-sections oriented back-to-back forming an I-shaped cross section. For each specimen, the studs were connected to each other with two self-drilling screws spaced at a set distance. A track was connected running perpendicular to each end with a single self-drilling screw through each flange of the C-sections. The purpose of the track is to keep the ends of the studs together and represents a common end attachment. As a result of the investigation, the current design requirements were found to be conservative in predicting the ultimate capacity of built-up studs (Stone and LaBoube, 2005).

The American Iron and Steel Institute's *North American Specification for the Design of Cold-Formed Steel Structural Members* (AISI, 2012), AISI S100, stipulates design guidance for assemblies such as built-up compression members. The specification states for compression members composed of two sections in contact that the nominal axial strength, P_n , shall be calculated as follows:

$$P_n = A_e F_n \quad (1)$$

Where F_n is

For inelastic buckling, $\lambda_c \leq 1.5$

$$F_n = (0.658^{\lambda_c^2}) F_y \quad (2)$$

For elastic buckling, $\lambda_c > 1.5$

$$F_n = \left[\frac{0.877}{\lambda_c^2} \right] F_y \quad (3)$$

Where $\lambda_c = (F_y/F_e)^{1/2}$

$$F_e = \frac{\pi^2 E}{(KL/r)^2} \quad (4)$$

If the buckling mode produces shear forces in the connectors between the members, KL/r should be replaced with $(KL/r)_m$.

$$\left(\frac{KL}{r} \right)_m = \sqrt{\left(\left(\frac{KL}{r} \right)_o^2 + \left(\frac{a}{r_i} \right)^2 \right)} \quad (5)$$

Where A_e is effective area at the stress, F_n , F_e is least of the elastic flexural, torsional, and torsional-flexural buckling stress, E is modulus of elasticity, F_y is yield strength, K is effective length factor, L is unbraced length of member, $(KL/r)_o$ is overall slenderness ratio of entire section about built-up member axis, a is intermediate fastener spacing and r_i is minimum radius of gyration of full unreduced cross-sectional area of an individual shape in a built-up member.

An experimental study was performed at the UMR concentrating on the behavior of built-up compression members, specifically I-sections (Stone and LaBoube, 2005). The purpose of the investigation was to assess the behavior of the built-up cold-formed steel compression members and to determine if the present AISI S100 design methodology is valid for cold-formed steel members.

The Structural Stability Research Council Technical Memorandum No. 4: Procedure for testing centrally loaded columns (Galambos, 1998) provided basic guidance for the development of the experimental study.

Specimens tested in this investigation were constructed of C-shaped sections oriented back-to-back with edge stiffened flanges and track sections. Figs. 1 and 2 illustrate typical C- and track sections used in this study. All column specimens were nominally seven feet tall and the cross-section parameters of the C-sections used in this study varied as follows:

- Thickness, t : 0.84 mm – 1.37 mm
- Depth, D : 92 mm – 152 mm
- Flange, b_f : 41.3 mm
- Edge Stiffener, d_f : 9.53 mm
- Screw Spacing, a : 305 mm – 914 mm

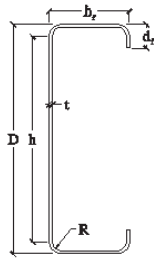


Figure 1. Typical C-Section Parameters

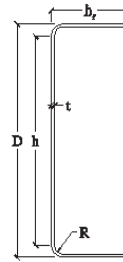


Figure 2. Typical Track Section Parameters

The built-up compression members were tested in a universal testing machine as shown by Fig. 3.



Figure 3. Test Setup



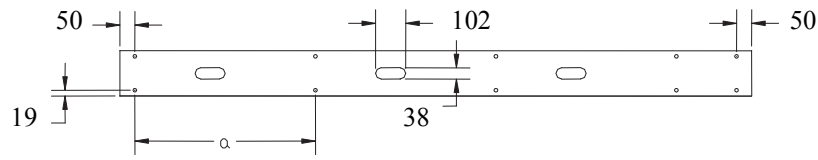
Figure 4. Bottom Pin Connection

Simulated pin-pin end connections were used in an attempt to achieve an effective length factor of unity. The bottom connection is illustrated in Fig. 4. The pin connection at the top of the stud was similar to the bottom connection in that the two plates had the same half-hemisphere. However, the upper plate in the top connection was connected to a load cell.

The two C-sections were fastened together with screws through the web starting 50 mm from one end and 19 mm from the inside of the flange. The screw spacing, a , was varied for the test specimen, using spacing values of 305 mm, 610 mm, and 914 mm. The typical screw layout is illustrated in Figs. 5 and 6.

A 305 mm long track section was screw attached to each end of the built-up I-section to simulate a typical industry application (Fig. 4).

The load application consisted of centering the stud in the test fixture and applying a compression load through the center of gravity of the built-up member. The ultimate failure load, P_{test} , was defined as when the test specimen was no longer capable of sustaining additional load. Table 1 summarizes the failure loads. Although each test specimen was loaded until failure, some of the specimens experienced local buckling, but continued to carry load until the stud formed a smooth curvature with the flanges buckling near mid-span and eventually failed as shown in Fig. 7.



$a = 305, 610, 914 \text{ mm}$

Figure 5. Schematic of Screw Spacing and Layout



Figure 6. Typical Screw Spacing and Layout



Figure 7. Typical Failure Mode

The recorded failure load, P_{test} , for the 32 tests was first compared to the unmodified predicted failure load, P_n , as determined by Section C4 of the AISI S100 without using the (KL/r) modification. Figure 8 illustrates the comparison of P_{test}/P_n .

Fig. 8 indicates that for the thicker materials the existing AISI design equations without using the modified slenderness ratio (Eq. 5) are conservative by an average of 43%. This suggests that the modification is not necessary for the thicker materials. The capacity of the thinner material (0.89 mm) was slightly overestimated by an average of 1%, with five of the fourteen values being less than one.

The recorded failure load, P_{test} , for the 32 tests was also compared against the modified predicted failure load, P_{nm} , as determined by Section C4 of AISI S100 using the (KL/r) modification (Eq. 5). Fig. 9 illustrates the comparison of P_{test}/P_{nm} .

Fig. 9 indicates for the thicker materials the existing AISI design equations including the modified slenderness ratio (Eq. 5) are conservative by an average of 65%. This suggests that the modification is not necessary for the thicker materials. The capacity of the thinner material (0.89 mm) was overestimated by an average of 16%; with only two of the P_{test}/P_{nm} values less than one. The test data indicates that the existing design specification provisions pertaining to the application of the modified slenderness ratio may be applicable for thinner members only. However, for all thicknesses, the AISI S100 stringent end fastener requirements are not warranted.

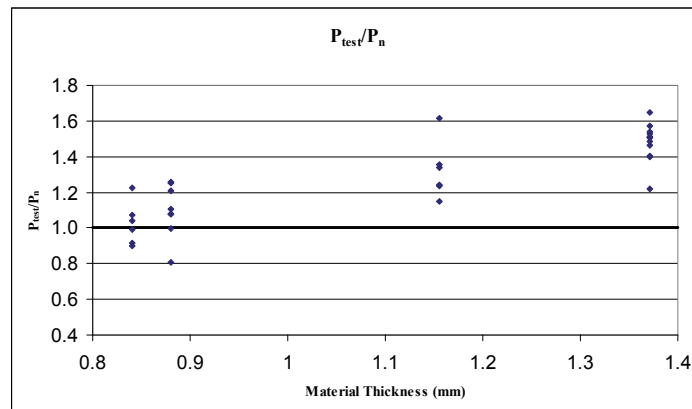


Figure 8 Test versus Computed Strength Using the Unmodified KL/r

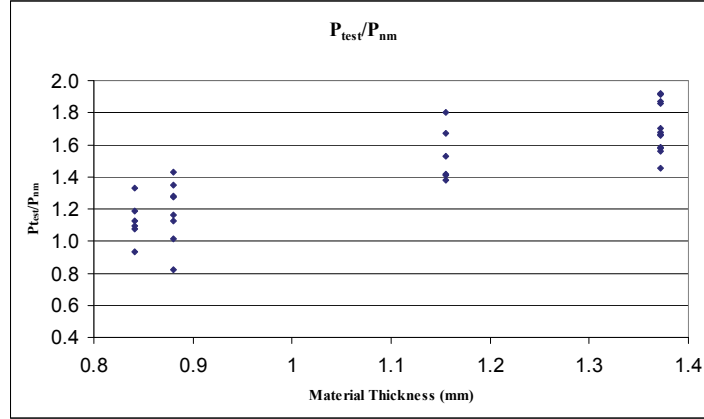


Figure 9 Test versus Computed Strength Using the Modified KL/r

3. Cold-Formed Steel Trusses

In the United States, cold-formed C-sections are commonly used as roof truss members. The use of singly-symmetric sections and the connection arrangements used result in development of bending effects in addition to axial loads in compression web members. At UMR, experimental work was carried out on full-scale trusses. The purpose of the research was to study the behavior of cold-formed C-section truss chord and web members and to develop appropriate design recommendations. A brief summary of the experimental studies and their findings are presented.

3.1 Web Members

The objective of the UMR experimental study was to evaluate the strength of the compression web truss members, to study their structural behavior and failure mode, and to develop a valid analytical model for analysis and design. A series of 20 tests fabricated using 64 mm deep C-sections with thicknesses of 0.91, 1.19 or 1.40 mm were carried out on full-scale truss assemblies (Ibrahim et al., 1997). All of the trusses were fabricated using single C-sections and self-drilling screws. The length of the compression webs were chosen to provide slenderness ratios (L/r) of 100, 150 and 180.

The maximum observed total truss vertical applied loads, at failure of the compression web, for each truss, W_{test} , are presented in Table 2. Failure of compression web was defined either by bending failure or when the transverse deflections became unstable. In no case did the compression web show a torsional behavior.

The predicted total vertical load applied on each truss was calculated for two different load conditions. First, using the nominal axial load capacity for a concentrically loaded compression web member as the limiting load capacity, the total load on the truss, W^* , was determined. The total load on the truss, W , was also computed by using Eq. 6. When evaluating Eqn. 6, P_n^* was taken as the nominal flexural buckling capacity.

$$\frac{P}{P_n^*} + \frac{C_m(Pe)}{M_{ny} \cdot \alpha_y} \leq 1.0 \quad (6)$$

Where P is the applied axial load, P_n^* is the nominal axial load, C_m is end moment coefficient, e is distance from centroid to outer edge of sections web, M_{ny} nominal bending strength about the minor axis, $1/\alpha_y$ second order effect factor.

Generally, W_{test} exceeded W but was less than W^* . Thus, Eq. 6 underestimated the load carrying capacity of the web member, but ignoring the combined axial and bending behavior would be unconservative. This load correlation may be attributed to two conditions. First, the compression webs were observed to behave as beam-columns, not concentrically axially loaded members. Second, the eccentric nature of the load application forced a dominant the minor axis flexural buckling behavior. Therefore, flexural-torsional buckling was not a possible failure mode.

The ratios between predicted and observed compression member axial loads P/P_{test} (Table 2) also indicate a conservative trend. P is the computed axial load in the compression web when the truss is subjected to total vertical load W and P_{test} is the computed axial load at W_{test} . For Test Nos. 2, 3, and 8, the ratio P/P_{test} was equal to 0.65, 0.64, and 0.57 respectively although different top chord rotational restraint conditions existed. Test Nos. 1 through 8 had an average ratio P/P_{test} of 0.56, while the same average for Test Nos. 9 to 13 was 0.61 although different top chord stiffness existed. Therefore, it may be concluded that neither the rotational restraint conditions of the top chord nor its flexural stiffness had a significant effect on the capacity of the compression web.

A review of the data indicated that the ratios of P/P_{test} (Table 2) seem to be related to the slenderness ratio L/r . Average values of P/P_{test} for test specimens having $L/r = 100$ was equal to 0.58, with a standard deviation of 0.062, while for test specimens having $L/r = 150$ and $L/r = 180$ the average P/P_{test} ratio was 0.74, with a standard deviation of 0.081. Modification of Eq. 6 was suggested as follows:

$$\frac{f \cdot P}{P_n^*} + \frac{C_m (f \cdot P e)}{M_{ny} \cdot \alpha_y} \leq 1.0 \quad (7)$$

Where f is a reduction factor to account for the trend of P/P_{test} (Table 3), and is a function of L/r . For L/r between 100 and 180, the reduction factor f may be computed using Eqn. 8

$$f = - \left(\frac{L/r}{173} \right)^2 + \frac{L/r}{88} - 0.22 \leq 0.8 \quad (8)$$

The last column in Table 2 shows the interaction values computed using Eq. 8. Considering the fact that in four tests, failure in the web member couldn't be achieved (Test Nos. 2, 3, 12 and 16) and in another four tests, the web member was capable of resisting more loads but with excessive deflections (Test Nos. 14, 15, 19, and 20), it can be concluded that Eqn. 8 can be used safely for the design of compression web members.

3.2 Top Chord Concentrated Loading

The objective of this phase of the UMR experimental study (Ibrahim et al., 1997) was to explore the structural behavior and the failure mode of the top chord members under concentrated loads, and to develop a valid analytical model for the analysis and design. A series of twenty-eight tests was carried out on full-scale truss assemblies.

All of the trusses were fabricated using C-sections and self-drilling screws. Eight different profiles of top chord cross-sections were tested. Each profile type had different material thickness and mechanical properties. Concentrated load bearing lengths, N , of 51 and 102 mm were used at the intermediate panel point.

All trusses were load until failure. For 24 of the 28 tests, web crippling failures were observed at the intermediate panel point of the top chord.

An interaction formula was suggested in order to recognize the combined action of axial compression, bending moment, and web crippling that caused top chord failure at the points of load application. The total interaction, I , is calculated as follows:

$$I = \frac{P}{P_{no}} + \frac{M_x}{M_{nx}} + \frac{R}{R_n} \quad (9)$$

Where P_{no} is nominal axial load fully braced compression member, M_x applied bending moment about the x-axis, M_{nx} is the nominal bending strength about the x-axis, R is the applied panel point concentrated load and R_n is the nominal interior one-flange loading condition web crippling strength for a single web.

Equation 9 is based on the common form of interaction equations of combined axial compression and bending and combined bending and web crippling. Values of total interaction, "I" were computed by Eq. 6 for each truss assembly at the failure load. Values of I ranged from 1.27 to 1.77 with an average value of 1.49 and a standard deviation of 0.12.

3. Header Beams

To span openings header beams are commonly used in bearing walls framed with cold-formed steel studs. Presented are the results of an experimental study conducted at the UMR to establish the web crippling strength of both box- and I-beam headers for an interior-one-flange (IOF) loading condition (Stephens and LaBoube, 2003). The header beam specimens were tested as a system consisting of two C-sections together with attached top and bottom track sections. The header configurations used in this study are defined in the *North American Standard for Cold-Formed Steel Structural Framing* (American, 2015). Tested as a system, it was found that the web crippling strength was greater than that for two independent, single web C-sections. Based on the results of this study design recommendations were proposed.

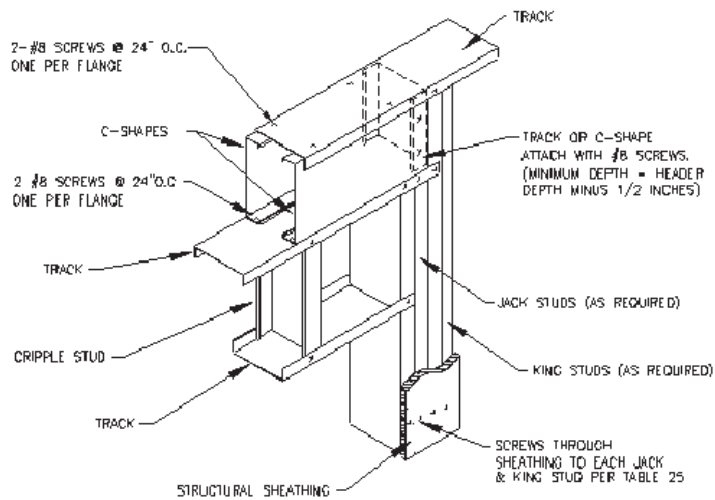


Figure 10 Box-Beam Header

The experimental investigation focused on testing of box-beam headers constructed as shown in Fig. 10. All specimens were fabricated using industry standard material provided by three different manufactures of cold-formed steel construction products.

A total of 38 box-beam specimens were tested with either a single-point or multiple-point loading as illustrated by Fig. 11. The length of bearing for the beam end reactions was 3-inches (76 mm) and 1 1/2-inches (38 mm) for the IOF load points. Figure 11 shows a schematic of a test set-up for a specimen with two IOF load points.

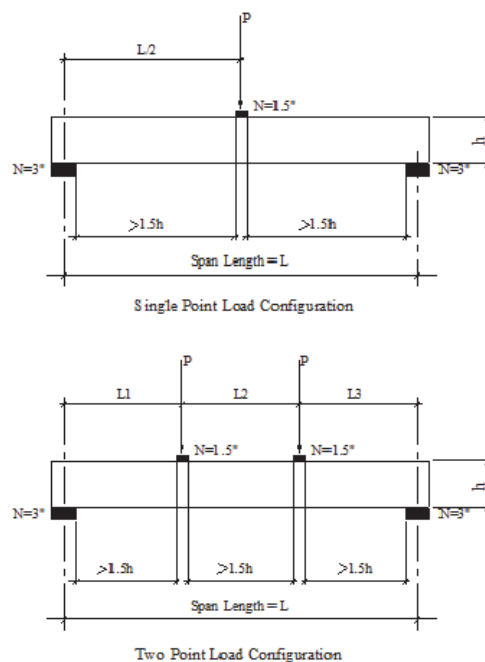


Fig. 11 Typical Test Specimen Loading Configurations

For the box-beam specimens, based on analysis of the test results, it was determined that the ratio of track thickness to C-section thickness were key parameters that contributed to the increased web crippling strength of the box-beam header specimens and is represented by the following relationship between P_t/P_n and C-section to track thickness:

$$\frac{P_t}{P_n} = 2.3 \left(\frac{t_c}{t_t} \right) \quad (10)$$

Where P_n is the web crippling strength computed by using the AISI S100 equation, t_c is thickness of C-section and t_t is thickness of top track.

4. Conclusions

To achieve more economical cold-formed steel solutions for the construction industry the future research efforts should focus on the behavior of assemblies. This paper summarized past research efforts that focused on the behavior of assemblies.

For built-up compression members, a total of 32 specimens were tested for this study. An analysis of the data determined that for thicker materials the currently applied modified slenderness ratio was not necessary when computing axial capacity, and therefore the designer can use the actual slenderness ratio of the built-up member. Analysis of the data also determined that existing design specification provisions pertaining to the modified slenderness ratio may be followed when designing thinner members. However, for all thicknesses, the AISI S100 stringent end fastener requirements are not warranted.

The UMR research on cold-formed steel trusses focused on developing a better understanding of the behavior of truss assemblies. Based on the research findings, appropriate design recommendations were developed for both chord and web members.

The objective of the box-beam header experimental study was to develop a design methodology for conventionally framed box-beam headers subject to interior-one-flange web crippling loads. This was accomplished by experimental tests of headers as an assembly composed of two C-sections and two track sections. Based on the tests carried out for this study, the nominal web crippling strength for box-beam headers can be determined by using the AISI S100 web crippling equation with a modifier that depends upon the thickness of the top track and the C-sections.

Acknowledgments

My success as a educator and researcher was possible because of the great mentors who guded me and the great students and collaborators who made the journey so enjoyable.

My introduction to stability research began with my Ph.D. study on the behavior of cold-formed steel web elements subject to bending, shear and the combination of bending and shear. It was my Ph.D. advisor, Dr. Wei-Wen Yu, who taught me to always study research data and ask “What is the data teaching us?” Dr. Yu instilled in me an interest in cold-formed steel structures and their unique stability challenges. Thank you Dr. Yu!

During my career I have been fortunate to have participated in countless cold-formed steel industry activities that enabled me to benefit from interactions with many engineers who have made substantial contributions to the cold-formed steel industry. Thank you members of the AISI Committee on Specifications and Committee on Framing Standards!

The research work reported herein was conducted at the Department of Civil Engineering of the University of Missouri-Rolla (now Missouri University of Science and Technology). I extend appreciation to the following graduate students whose work is summarized in this paper: Dr. T. M. Ibrahim, M. M. Harper, J. A. Riemann, Dr. S.F. Stephens, and T.A. Stone. Thanks are also due to the laboratory support staff of the Department of Civil Engineering, Mr. J. Bradshaw, Mr. J. McCracken, Mr. S. Gable, Mr. B. Swift, and Mr. G. Abbott for their assistance.

Huge thanks goes to Ms. Christina Stratman, Administrative Assistant, who assisted me with this manuscript and many previous manuscripts, conference proceedings and CCFSS projects.

Finally, a very special thank you to my wife, Karen, and my daughters, Jennifer and Elizabeth, for your support and understanding especially when, on many evenings, I withdrew to my office instead of spending the evening with you. I love you!!

References

- American Iron and Steel Institute (2012). "North American Specification for the Design of Cold-Formed Steel Structural Members," AISI S100, Washington, D.C.
- American Iron and Steel Institute (2015), "North American Standard for Cold-Formed Steel Structural Framing", AISI S240, Washington, D.C.
- Galambos, T. V. (Editor) (1998). "Guide to Stability Design Criteria for Metal Structures," Fifth Edition, John Wiley and Sons, Inc, New York, NY
- Ibrahim, T.M., Riemann, J.A., LaBoube, R.A. and Yu, W.W. (1997), "Behavior of Compression Web Members of Cold-Formed Steel Roof Trusses," Proceedings of the International Conference on Experimental Model Research and Testing of Thin-Walled Structures, Prague
- Stephens, S.F., and LaBoube, R.A. (2003), "Web Crippling and Combined Bending and Web Crippling of Cold-Formed Steel Beam and Headers," *Thin-Walled Structures*, 41 (2003), Elsevier Ltd.
- Stone, T.A. and LaBoube, R.A. (2005), "Behavior of Cold-Formed Steel Built-Up I-Sections," *Thin-Walled Structure*, 43 (2005), Elsevier Ltd.

Table 1 Built-Up Compression Member Test Results

| Measured Thickness (mm) | Section Depth (mm) | Screw Spacing, a (mm) | P _{test} (kN) |
|-------------------------|--------------------|-----------------------|------------------------|
| 1.372 | 152 | 305 | 80.60 |
| 1.372 | 152 | 610 | 82.96 |
| 1.372 | 152 | 610 | 77.00 |
| 1.372 | 152 | 610 | 81.22 |
| 1.372 | 152 | 762 | 74.06 |
| 1.372 | 152 | 762 | 78.38 |
| 1.372 | 152 | 762 | 86.74 |
| 1.372 | 152 | 914 | 73.53 |
| 1.372 | 152 | 914 | 64.32 |
| 1.372 | 152 | 1016 | 79.36 |
| 1.372 | 152 | 1067 | 79.36 |
| 1.372 | 152 | 1067 | 79.80 |
| 1.155 | 92 | 305 | 55.29 |
| 1.155 | 92 | 305 | 66.90 |
| 1.155 | 92 | 610 | 51.24 |
| 1.155 | 92 | 610 | 51.15 |
| 1.155 | 92 | 914 | 47.55 |
| 1.155 | 92 | 914 | 55.96 |
| 0.880 | 92 | 305 | 42.75 |
| 0.880 | 92 | 305 | 37.63 |
| 0.880 | 92 | 305 | 27.40 |
| 0.880 | 92 | 305 | 33.85 |
| 0.880 | 92 | 610 | 36.65 |
| 0.880 | 92 | 610 | 42.48 |
| 0.880 | 92 | 914 | 36.65 |
| 0.880 | 92 | 914 | 41.06 |
| 0.841 | 152 | 305 | 32.69 |
| 0.841 | 152 | 305 | 38.21 |
| 0.841 | 152 | 610 | 43.81 |
| 0.841 | 152 | 610 | 37.05 |
| 0.841 | 152 | 914 | 32.03 |
| 0.841 | 152 | 914 | 35.32 |

Table 2
Truss Observed vs Computed Loads

| Test No. | W_{test} | Predicted Failure Loads(kN) | | Axial Loads in Web Members (kN) | | P/P_{test} | Interaction Values | | |
|----------|------------|-----------------------------|-------|---------------------------------|------------|--------------|--------------------|---------|------|
| | | W· | W | P | P_{test} | | Eqn (6) | Eqn (8) | |
| 1 | 24.75 | 30.38 | 11.84 | 8.60 | 17.98 | 0.48 | 3.06 | 1.28 | |
| 2 | 29.25 | 48.24 | 19.04 | 14.31 | 22.01 | 0.65 | 2.07 | 0.86 | |
| 3 | 29.97 | 48.24 | 19.04 | 14.31 | 22.50 | 0.64 | 2.17 | 0.89 | |
| 4 | 34.20 | 48.24 | 19.04 | 14.31 | 25.70 | 0.56 | 3.05 | 1.07 | |
| 5 | 40.86 | 58.32 | 23.76 | 18.23 | 31.41 | 0.58 | 2.89 | 1.00 | |
| 6 | 38.66 | 48.24 | 19.04 | 14.31 | 29.03 | 0.49 | 4.76 | 1.28 | |
| 7 | 36.99 | 48.24 | 19.04 | 14.31 | 27.77 | 0.51 | 3.95 | 1.20 | |
| 8 | 29.70 | 48.24 | 19.04 | 14.31 | 24.89 | 0.57 | 2.78 | 1.02 | |
| 9 | 15.75 | 22.95 | 8.96 | 8.60 | 15.21 | 0.57 | 2.24 | 1.04 | |
| 10 | 14.58 | 22.95 | 8.96 | 8.60 | 14.04 | 0.61 | 1.97 | 0.94 | |
| 11 | 15.62 | 22.95 | 8.96 | 8.60 | 15.08 | 0.57 | 2.21 | 1.03 | |
| 12 | 13.82 | 22.95 | 8.96 | 8.60 | 13.32 | 0.65 | 1.81 | 0.88 | |
| 13 | 13.32 | 22.95 | 8.96 | 8.60 | 12.83 | 0.67 | 1.71 | 0.84 | |
| 14 | 6.35 | 11.25 | 5.09 | 5.60 | 7.47 | 0.80 | 1.42 | 0.88 | |
| 15 | 9.59 | 14.04 | 7.29 | 8.64 | 11.39 | 0.76 | 1.71 | 0.95 | |
| 16 | 11.43 | 16.70 | 9.00 | 10.76 | 13.64 | 0.79 | 1.58 | 0.89 | |
| 17 | 14.31 | 16.70 | 9.00 | 10.76 | 16.92 | 0.63 | 3.85 | 1.31 | |
| 18 | 8.73 | 10.22 | 6.03 | 4.82 | 7.92 | 0.61 | 3.24 | 1.45 | |
| 19 | 9.14 | 11.52 | 7.47 | 6.57 | 8.28 | 0.79 | 1.53 | 0.89 | |
| 20 | 11.34 | 13.68 | 9.05 | 6.24 | 10.62 | 0.78 | 1.70 | 0.94 | |
| Average | | | | | | 0.64 | 2.49 | 1.03 | |
| | | | | | | | Standard Deviation | | 0.18 |